



ASYMMETRY PARAMETERS OF THE PHASE FUNCTION FOR DENSELY PACKED SCATTERING GRAINS

MICHAEL I. MISHCHENKO

NASA Goddard Institute for Space Studies, Hughes STX Corporation, New York, NY 10025, U.S.A.

(Received 13 September 1993)

Abstract—Spatial correlation among densely packed particles can substantially change their single-scattering properties, thus making questionable the applicability of the independent scattering approximation in calculations of light scattering by planetary regoliths. The same problem arises in geophysics in light scattering computations for snow, frosts, and bare soil. In this paper, we use a dense-medium light-scattering theory based on the introduction of the static structure factor to calculate asymmetry parameters of the phase function for densely packed particles with real refractive indices 1.31 and 1.66, approximating water ice and soil particles, respectively, and imaginary refractive indices 0, 0.01, and 0.3. For sparsely distributed, independently scattering grains, the calculated asymmetry parameters are always positive and always larger than those for densely packed particles. For densely packed particles, the asymmetry parameters may be negative but only for radius-to-wavelength ratios from about 0.1 to about 0.4. With decreasing particle size, the calculated asymmetry parameters tend to zero independently of the compaction state. In the geometrical optics regime, the asymmetry parameters for densely packed scatterers are positive and very close to those for independently scattering grains. These results may have important implications for remote sensing of the Earth and solid planetary surfaces. In particular, it is demonstrated that negative asymmetry parameters derived with some approximate multiple-scattering theories may be physically irrelevant and can be the result of using an inaccurate bidirectional reflection function combined with the ill-conditionality of the inverse scattering problem.

1. INTRODUCTION

It is usually assumed that the surfaces of most atmosphereless bodies in the solar system are particulate media composed of densely packed regolithic grains.^{1–3} In such densely packed media, spatial correlation among particles can result in substantial changes of their single-scattering properties (such as optical cross sections and phase function), thus making questionable the applicability of the independent scattering approximation^{4,5} in calculations of light scattering by planetary regoliths. The same problem arises in geophysical calculations of light scattering by snow, frosts, and bare soil.^{6–10} Therefore, rigorous dense-medium theories must be used to examine the effects of packing density on light scattering.

An especially interesting quantitative characteristic of scattering particles is the asymmetry parameter of the phase function. Indeed, unlike the extinction and scattering cross sections, which may also be changed by effects of packing density, the asymmetry parameter can change not only its absolute value, but also its sign. It is well known that even small changes in the absolute value of the asymmetry parameter, to say nothing of the reversal of its sign, can significantly affect the thermal regime of the scattering medium.^{11,12} Therefore, accurate calculations of the asymmetry parameter are especially important in computing the albedo of snow and ice^{6–10} and studies of the solid-state greenhouse effect in icy regoliths.¹³ Also, some approximate bidirectional reflection functions, when used to interpret photometric observations of the Earth and solid planetary surfaces, systematically give negative asymmetry parameters for regolithic and soil particles.^{1,3,14} Since asymmetry parameters for independently scattering dielectric grains are always nonnegative, it is important to verify whether those approximate reflection functions were accurate enough to give physically relevant results.

In this paper, we study how the asymmetry parameter of the phase function is changed depending on the compaction state of scattering particles. In our calculations, we use a dense-medium light-scattering theory based on introducing the so-called static structure factor.¹⁵ In the following section, we briefly recapitulate the main formulas of this theory and present and analyze theoretical calculations of the asymmetry parameter for a representative selection of particle refractive indices, radius-to-wavelength ratios, and compaction states. In Section 3, we discuss implications of our calculations for remote sensing of the Earth and solid planetary surfaces. The results of the paper are summarized in the concluding section.

2. CALCULATIONS

For sparsely distributed, independently scattering particles, the asymmetry parameter of the phase function g is defined as the mean cosine of the scattering angle:^{4,5}

$$g = \langle \cos \theta \rangle = 1/2 \int_{-1}^1 d(\cos \theta) p(\theta) \cos \theta, \quad (1)$$

where θ is the scattering angle and $p(\theta)$ is the single-scattering particle phase function. Theoretically, the asymmetry parameter can vary from -1 to $+1$ and is negative for backscattering grains, positive for forward-scattering grains, and zero for isotropic scatterers.^{4,5} The phase function is given by

$$p(\theta) = \frac{4\pi}{C_{\text{sca}}} \frac{dC_{\text{sca}}}{d\Omega}, \quad (2)$$

where $dC_{\text{sca}}/d\Omega$ is the differential scattering cross section⁵ and

$$C_{\text{sca}} = \int_{4\pi} d\Omega \frac{dC_{\text{sca}}}{d\Omega} \quad (3)$$

is the total scattering cross section.

Densely packed regolithic and soil particles are not independent scatterers. Therefore, the concept of the single-scattering phase function cannot be used in the same sense as it is used in computations of light scattering by cloud and aerosol particles. However, the concept of the single-scattering phase function can still be used with some modification to calculate the intensity of light singly scattered by a layer of densely packed grains.^{15–18} Specifically, the angular distribution of the first-order-scattering contribution to the reflected intensity is given by that of the conventional radiative transfer theory provided that the differential scattering cross section is equal to the product of the independent-scattering differential cross section and so-called static structure factor $S(\theta)$. Thus, instead of Eqs. (1)–(3), we have for densely packed grains

$$p(\theta) = \frac{4\pi}{C_{\text{sca}}} \frac{dC_{\text{sca}}}{d\Omega} S(\theta), \quad (4)$$

$$C_{\text{sca}} = \int_{4\pi} d\Omega \frac{dC_{\text{sca}}}{d\Omega} S(\theta), \quad (5)$$

and

$$g = \frac{\int_{4\pi} d\Omega \frac{dC_{\text{sca}}}{d\Omega} S(\theta) \cos \theta}{\int_{4\pi} d\Omega \frac{dC_{\text{sca}}}{d\Omega} S(\theta)}. \quad (6)$$

Note that the theory based on the introduction of the static structure factor has a rather strong physical background and is based, in the last analysis, on solving Maxwell's equations for calculating light scattering and on statistical mechanics for describing the statistics of mutual positions of densely packed grains. In addition, Wolf et al¹⁹ and Saulnier et al²⁰ have found that this theory is in good quantitative agreement with results of their controlled laboratory experiments.

Thus to calculate the single-scattering phase function for densely packed particles, we must first compute the static structure factor. In general, this quantity depends on scattering angle and particle size distribution and shape.

Since the problem of computing the static structure factor for arbitrary particle size distribution and shape is extremely difficult, we have to make two usual approximations.¹⁵ Specifically, we assume scattering particles to be nearly spherically shaped and nearly monodisperse (the range of sizes is narrow compared with the mean grains size). It has been derived that for hard, impenetrable, monodisperse spheres of a radius r_0 , the structure factor in the Percus–Yevick approximation is given by¹⁵

$$S(\theta) = \frac{1}{1 - nC(p)}, \quad (7)$$

where

$$p = [4\pi \sin(\theta/2)]/\lambda, \quad (8)$$

n is the number density of scattering particles, λ is the wavelength of light, and $C(p)$ is given by¹⁷

$$C(p) = 24 \frac{f}{n} \left[\frac{\alpha + \beta + \delta}{u^2} \cos u - \frac{\alpha + 2\beta + 4\delta}{u^3} \sin u - \frac{2(\beta + 6\delta)}{u^4} \cos u + \frac{2\beta}{u^4} + \frac{24\delta}{u^5} \sin u + \frac{24\delta}{u^6} (\cos u - 1) \right], \quad p \neq 0 \quad (9)$$

and²¹

$$C(0) = -24 \frac{f}{n} \left(\frac{\alpha}{3} + \frac{\beta}{4} + \frac{\delta}{6} \right). \quad (10)$$

In Eqs. (9) and (10),

$$u = 2pr_0, \quad (11)$$

$$\alpha = \frac{(1 + 2f)^2}{(1 - f)^4}, \quad (12)$$

$$\beta = -6f \frac{(1 + f/2)^2}{(1 - f)^4}, \quad (13)$$

$$\delta = \alpha f/2, \quad (14)$$

where

$$f = \frac{4}{3} \pi n r_0^3 \quad (15)$$

is the filling factor (i.e., the fraction of a volume occupied by the particles). Note that for sparsely distributed grains ($n = 0$), the structure factor is identically equal to unity.

In Fig. 1 the static structure factor is shown as a function of the parameter u for six values of the filling factor. It is seen that increasing packing density results in an angular redistribution of the scattered intensity. The influence of packing density is especially significant at $u \lesssim 5$, i.e., at scattering angles $\theta \lesssim 0.4\lambda/r_0$. It is well known that the half-width at half-maximum of the forward-scattering cone due to diffraction of light on an isolated particle is given by $\theta \approx 0.25\lambda/r_0$. Thus, the main effect of increasing packing density is to suppress the forward-scattering diffraction component of the phase function. It should be noted that in the approximate multiple-scattering theories by Hapke and Lumme and Bowell,³ it is *a priori* assumed that, for particles in intimate contact, the phase function does not include the diffraction term. Figure 1 enables one to quantify the validity of this assumption and shows that it becomes reasonably accurate only for filling factors exceeding roughly 0.2.

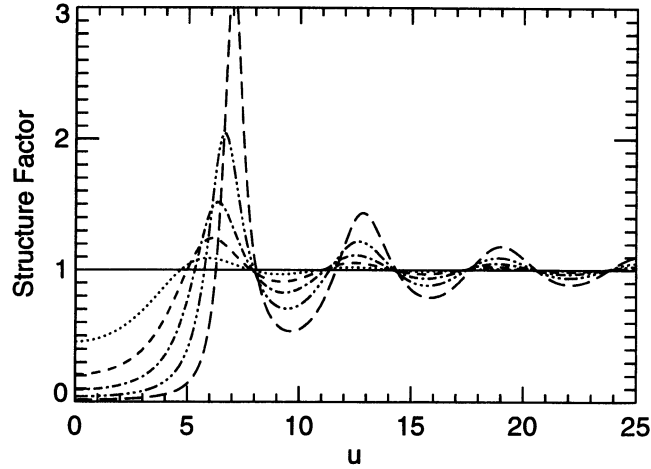


Fig. 1. Structure factor S vs parameter u for filling factors $f=0$ (solid line), 0.1 (dotted line), 0.2 (short-dashed line), 0.3 (dot-dashed line), 0.4 (triple-dot-dashed line), and 0.5 (long-dashed line).

In Figs. 2–7, we present results of numerical computations of the asymmetry parameter for two values of the real part and three values of the imaginary part of the refractive index and six values of the filling factor. Note that the real refractive index 1.31 is close to that of water ice while the value 1.66 approximates the real refractive index of soil particles²² and the mineral enstatite at visible wavelengths. Asymmetry parameters are plotted vs a dimensionless ratio $y = r_0/\lambda$. In these computations, we used the Mie scattering theory^{4,5,23,24} to calculate the differential scattering cross section for independently scattering spherical particles of a given size and refractive index and then employed a Gaussian quadrature formula to evaluate the integrals in Eq. (6) numerically for different values of the filling factor f . Note that to obtain convergent results for large particles and large filling factors, the number of Gaussian division points should be of order of several thousand. It is well known that monodisperse Mie quantities as a function of size parameter contain a high-frequency ripple which is usually suppressed in practice because, in nature, there is always a dispersion of grain sizes.^{4,5,23} Therefore, following Wiscombe and Warren,⁷ we reduced the ripple by averaging the asymmetry parameter over a range of sizes which was small relative to the mean grain size.

It is seen from Figs. 2–7 that for sparsely distributed, independently scattering spheres ($f=0$), the calculated asymmetry parameters are always positive and always larger than those for densely

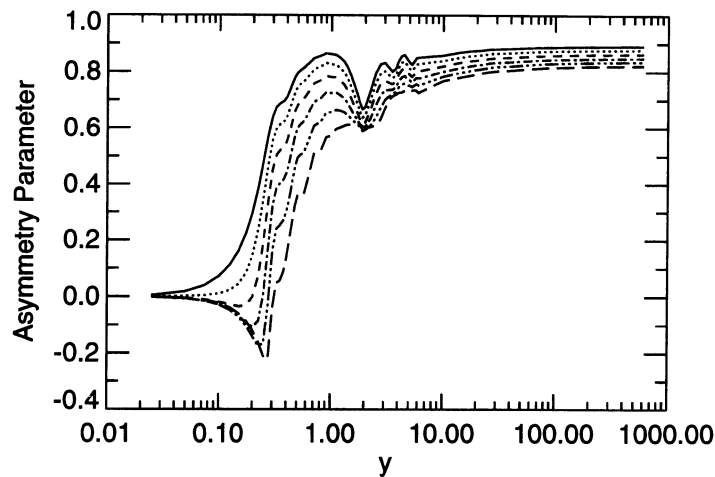


Fig. 2. Asymmetry parameters of the phase function vs radius-to-wavelength ratio y for spherical particles with refractive index 1.31 and filling factors $f=0$ (solid line), 0.1 (dotted line), 0.2 (short-dashed line), 0.3 (dot-dashed line), 0.4 (triple-dot-dashed line), and 0.5 (long-dashed line).

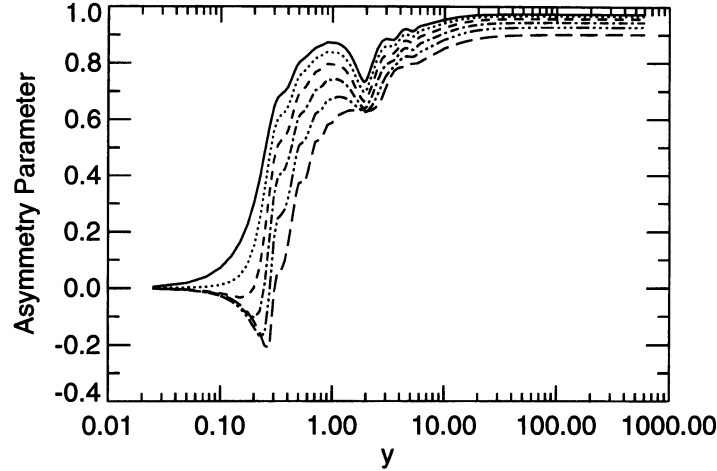


Fig. 3. As in Fig. 2, for refractive index $1.31 + 0.01i$.

packed grains. With decreasing particle size, the asymmetry parameters tend to zero independently of the compaction state. For particles much larger than the wavelength, the asymmetry parameters for densely packed particles are positive and very close to those for independently scattering spheres despite the fact that the effects of high packing density strongly suppress the forward-scattering diffraction peak (Fig. 1). Thus in the geometrical optics limit, the approximation of independent scattering gives reasonably good accuracy and may be used in practical computations for densely packed grains.^{7-10,25,26} The most interesting result of our calculations is that, unlike independently scattering particles, the asymmetry parameter for densely packed grains may be negative, but, irrespective of refractive index, only for radius-to-wavelength ratios in the range $0.1 \lesssim y \lesssim 0.4$.

Although calculations displayed in Figs. 2-7 have been performed for spherical particles, our observations summarized in the preceding paragraph are, apparently, valid for nonspherical particles and particles with rough surfaces as well. Indeed, Figs. 8 and 9 show asymmetry parameters for randomly oriented oblate spheroids and Chebyshev particles, respectively, rigorously calculated using the T-matrix method.²⁷⁻²⁹ The aspect ratio of the spheroids is 1.5, thus demonstrating effects of a major departure of particle shape from sphericity. The shape of the rotationally symmetric Chebyshev particles in the spherical coordinate system is governed by the equation³⁰

$$r(\vartheta, \phi) = R_0[1 + 0.05 \cos(8\vartheta)], \quad \vartheta \in [0, \pi], \quad \phi \in [0, 2\pi] \quad (16)$$

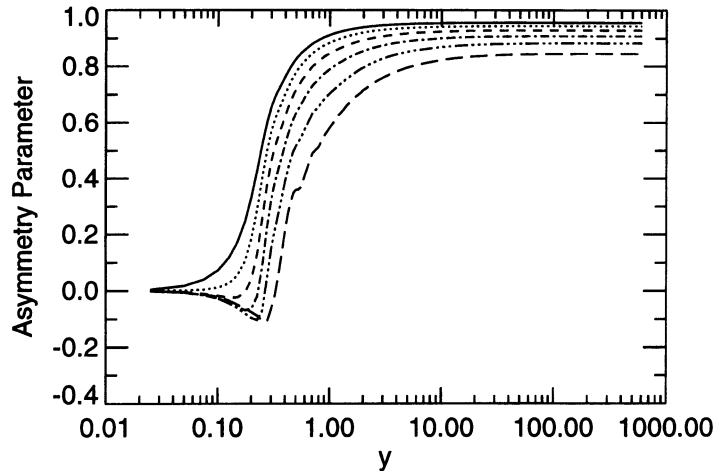


Fig. 4. As in Fig. 2, for refractive index $1.31 + 0.3i$.

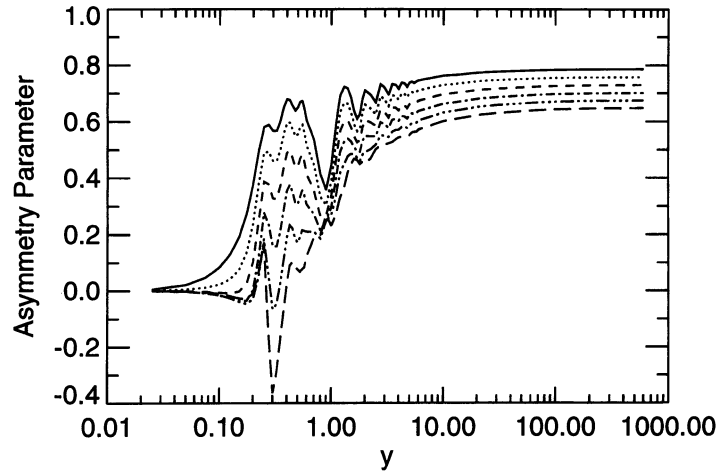


Fig. 5. As in Fig. 2, for refractive index 1.66.

and is the result of continuously deforming a sphere by means of the Chebyshev polynomial of degree 8, thus being ideally suited to model small-scale surface roughness of nearly-spherically shaped particles. Because of numerical limitations, calculations in Figs. 8 and 9 are shown for radius-to-wavelength ratios y not exceeding 10. However, Figs. 2–7 demonstrate that asymmetry parameters are most sensitive to y in the region $0.01 \lesssim y \lesssim 10$, and comparison of Figs. 3, 8, and 9 shows that in this region the effects of particle nonsphericity and surface roughness are small.

As was explained above, the dense-medium single-scattering phase function, as defined by Eq. (4), describes the first-order-scattering contribution to the reflected intensity and, as such, has a definite physical meaning. Moreover, for highly absorbing particles, for which the higher-order-scattering contribution to the reflected light is negligibly small, it becomes a directly observable quantity. Also, for nonabsorbing or slightly absorbing particles the dense-medium asymmetry parameter given by Eq. (6) specifies the photon transport mean free path and, therefore, can be determined from measurements of the angular width of the backscattering intensity peak and polarization opposition effect caused by weak localization of photons in discrete random media.^{19,21,31–33}

Of course, an interesting question is whether the classical independent-scattering phase function or the modified dense-medium phase function given by Eq. (4) can be used in the radiative transfer equation to calculate the multiple-scattering contribution to the reflected intensity for densely packed particles. It has been shown in Ref. 34 that the intensity (or, more generally, the Stokes

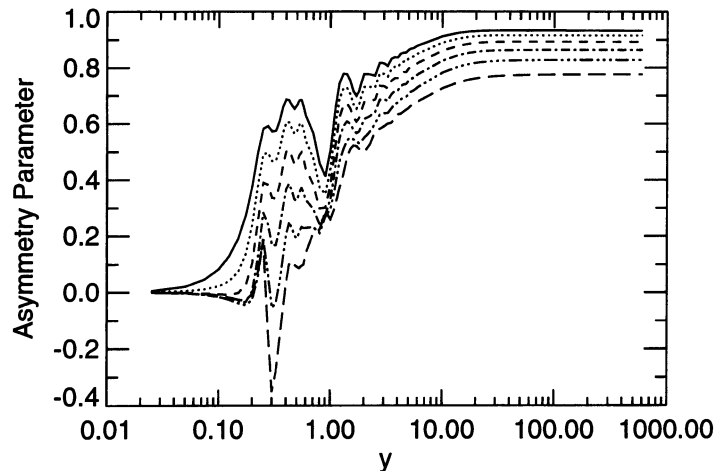


Fig. 6. As in Fig. 2, for refractive index $1.66 + 0.01i$.

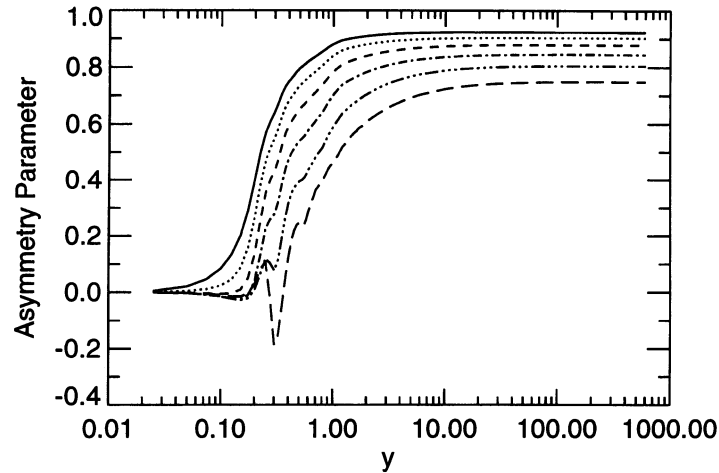


Fig. 7. As in Fig. 2, for refractive index $1.66 + 0.3i$.

vector) of light multiply scattered by densely packed particles with sizes much smaller than the wavelength (i.e., Rayleigh scatterers) is a solution of an equation which has the same form as the classical radiative transfer equation and contains exactly the same independent-scattering phase function (matrix), but the extinction coefficient and single-scattering albedo are modified. For a semi-infinite nonabsorbing (or weakly absorbing) medium, this modified radiative transfer equation gives exactly the same result as the classical radiative transfer equation. Therefore, the use of the classical radiative transfer equation is justified if the densely packed scattering particles are nonabsorbing or slightly absorbing and very small compared with the wavelength. Also, by comparing theoretical radiative transfer calculations with results of controlled laboratory experiments,^{19,35} it has recently been demonstrated³⁶ that the classical radiative transfer equation containing the independent-scattering phase function (matrix) gives good quantitative results for densely packed nonabsorbing particles with sizes comparable to and slightly larger than the wavelength. The filling factor in those experiments was as large as 0.1, while it is usually believed that the classical radiative transfer equation is valid only for filling factors smaller than roughly 0.001. Similar comparisons of radiative transfer computations with results of his controlled laboratory experiments for big transparent particles have been performed by Goguen.³⁷ It follows from Fig. 1 that the effect of packing density on the phase function at side- and backscattering

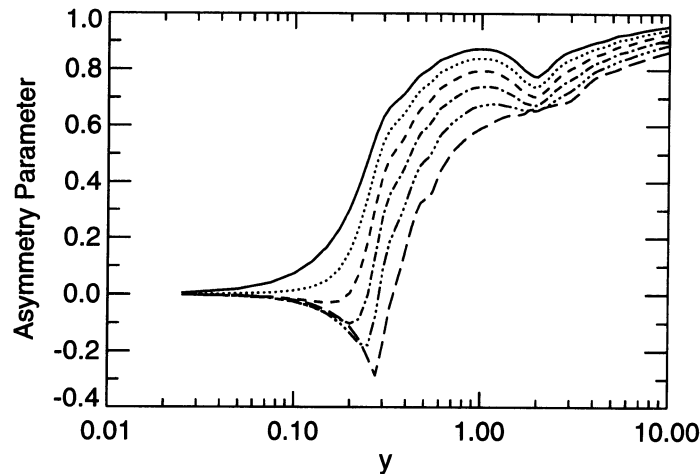


Fig. 8. Asymmetry parameters of the phase function vs the ratio of the equal-volume-sphere radius to the wavelength y for randomly oriented oblate spheroids with refractive index $1.31 + 0.01i$, aspect ratio 1.5, and filling factors $f = 0$ (solid line), 0.1 (dotted line), 0.2 (short-dashed line), 0.3 (dot-dashed line), 0.4 (triple-dot-dashed line), and 0.5 (long-dashed line).

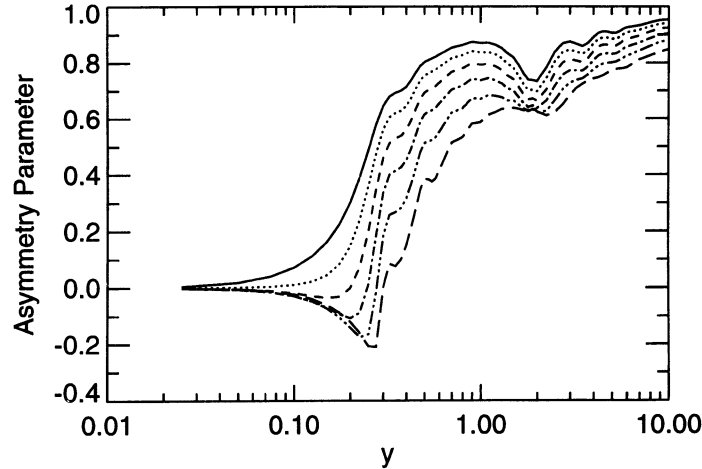


Fig. 9. As in Fig. 8, for randomly oriented Chebyshev particles with shape given by Eq. (16).

angles becomes negligibly small with increasing radius-to-wavelength ratio. Therefore, we may expect that the classical radiative transfer equation can give good results for big nonabsorbing or moderately absorbing particles. For example, the standard radiative transfer theory was used to compute the albedo of snow and frosts⁷⁻¹⁰ and to estimate the refractive index of soil particles.²² Also, in Ref. 38 a radiative transfer equation containing the classical independent-scattering phase matrix was used to compute millimeter-wave radar scattering from snow, in which case particles had sizes comparable to the wavelength of radiation. If particles are much larger than the wavelength and strongly absorbing, Monte Carlo ray-tracing modeling³⁹ may give good results.

3. IMPLICATIONS FOR REMOTE SENSING OF PLANETARY REGOLITHS AND SOIL PARTICLES

The Lumme and Bowel theory of light scattering by planetary regoliths^{3,40} implies a forward-scattering phase function of regolithic grains with a positive asymmetry parameter g and provides a reasonably good fit to observational data.³ On the other hand, the Hapke theory,⁴¹ when applied to the interpretation of photometric observations of atmosphereless planetary surfaces, including high albedo icy or ice-covered surfaces, gives an equally good fit but with systematically negative values of the asymmetry parameter of the single-scattering phase function (e.g., Refs. 1, 3, 42-46). This means that, when described by the Hapke model, the regolithic grains that form the particulate surfaces are backscattering. Similar negative asymmetry parameters have been derived applying the Hapke theory to soil particles.¹⁴ It is well known that independently scattering ice and soil particles have positive and usually large asymmetry parameters and are (strongly) forward scattering (Refs. 5, 7, 23, 29, 47-53 and Figs. 2-9). Therefore, to explain the negative values of the asymmetry parameter as inferred with the Hapke theory, it is usually hypothesized that particles become backscattering when they are densely packed.⁴¹ As follows from our calculations, this means that regolithic grains, regardless of their chemical composition and wavelength, must have radii in the range $0.1\lambda \lesssim r_0 \lesssim 0.4\lambda$. This seems absolutely unrealistic and contradicts the results of the study by Hapke and Wells⁵⁴ who applied the Hapke theory to interpret laboratory photometric measurements of particulate surfaces and obtained negative asymmetry parameters for glass particles much larger than the wavelength.

Another explanation of the negative asymmetry parameters obtained with the Hapke theory is that individual regolithic particles are in fact aggregates or chains of smaller grains and are multiple-scattering objects themselves. As a result of multiple scattering, these individual aggregates or chains scatter a significant fraction of light in the backscattering direction and thus cause a negative asymmetry parameter.^{44,55,56} However, if such composite particles are densely packed to

form a regolithic surface, the individual aggregates or chains become indistinguishable (there is no way to determine whether a grain is the last element of the previous chain or the first element of the next chain), and the light incident on the surface will “see” the scattering medium as a single superaggregate or superchain composed of the smaller grains. Thus, it is the smaller grains rather than the indistinguishable “individual” aggregates or chains that play the role of single scatterers. Therefore, they must be backscattering in themselves if the asymmetry parameters, as inferred with the Hapke theory, were indeed negative. This suggests once again that the smaller grains have sizes in the range $0.1\lambda \lesssim y_0 \lesssim 0.4\lambda$ irrespective of their composition and wavelength, which does not seem realistic.

One more explanation is that “individual” regolithic particles are filled with internal scatterers in the form of cracks, voids, and/or foreign inclusions and, as such, are multiple-scattering and, therefore, backscattering objects.⁵⁶ However, in densely packed regoliths the distance between internal scatterers belonging to the same “individual” particle is of the same order as or even greater than the distance between internal scatterers belonging to different adjacent “individual” regolithic particles. Therefore, multiple scattering of light by inclusions belonging to different “individual” particles can be stronger than that by inclusions belonging to the same “individual” particle. In other words, densely packed “individual” particles filled with foreign inclusions are no longer individual, separate multiple-scattering objects. It is the whole regolithic layer filled with internal scatterers which is the multiple-scattering object. Therefore, the Hapke single-scattering albedo and asymmetry parameter, which by definition are single-scattering quantities, must be associated with the primary single-scattering units in the form of cracks, voids, and/or foreign inclusions, which are forward-scattering. Another difficulty with this explanation is that it requires an unrealistically complicated internal structure for regolithic and soil particles as well as for glass particles used in laboratory experiments to validate the Hapke theory.⁵⁴

There is, however, another simple explanation of negative asymmetry parameters obtained with the Hapke theory which is based on the following two facts. First, several rather crude approximations have been made in the derivation of the Hapke bidirectional reflection function.⁴¹ For example, regardless of the actual phase function of regolithic particles, the contribution of photons scattered more than once is approximated in the Hapke theory by that of isotropic scatterers. As was shown by Goguen,³⁷ this approximation can significantly underestimate the actual contribution of multiply scattered photons for real phase functions. Also, the contribution of the first-order scattering is usually approximated by a single-peaked Henyey-Greenstein phase function or a few-term expansion in Legendre polynomials, which is too crude an approximation for most real phase functions. Second, it is well known that determination of the asymmetry parameter from measurements of the reflected light is an ill-conditioned inverse problem.^{57,58} This means that under certain conditions the reflected intensity can depend on the asymmetry parameter of the phase function rather weakly. As a result, experimental noise and/or approximations like those mentioned above can easily result in absolutely wrong values of the asymmetry parameter.⁵⁹

An example demonstrating the relevance of this latter explanation comes from Hapke and Wells.⁵⁴ Their Fig. 9 (reproduced then in Ref. 60) shows that, by using the Hapke bidirectional reflection function, they were able to obtain almost perfect fit to two relative brightness profiles of the Venus atmosphere, which was considered by the authors a corroboration of the adequacy of the model. However, their fit was obtained with an asymmetry parameter of the phase function equal to zero, whereas it is well known that Venus clouds are composed of micrometer-sized spherical droplets having strongly forward scattering phase functions with asymmetry parameters of about 0.7–0.8 in the visible.^{61,62} Thus, although the fit of the Hapke model to the observations was almost perfect, the inferred asymmetry parameter was absolutely wrong.

To further demonstrate our explanation of the origin of negative asymmetry parameters as inferred with the Hapke model, we rigorously calculated the bidirectional reflection function for a semi-infinite layer composed of sparsely distributed, strongly forward-scattering ice particles and then used the Hapke bidirectional reflection function to reconstruct the particle asymmetry parameter. To specify the single-scattering properties of the particles, we used a single-scattering albedo $\varpi = 1$ and a double-peaked Henyey-Greenstein phase function

$$p(\theta) = F \frac{1 - g_1^2}{(1 - 2g_1 \cos \theta + g_1^2)^{3/2}} + (1 - F) \frac{1 - g_2^2}{(1 - 2g_2 \cos \theta + g_2^2)^{3/2}} \quad (17)$$

with $g_1 = 0.85$, $g_2 = -0.8$, and $F = 0.98$, which reasonably accurately approximates the phase function measured in laboratory conditions for ice crystals with sizes of a few tens of micrometers.⁶³ Since we assumed the particles to be sparsely distributed and, thus, independently scattering, we used in our calculations the standard radiative transfer theory. Specifically, the bidirectional reflection function R was calculated by solving numerically the Ambartsumian nonlinear integral equation for R ⁶⁴ as described by Dlugach and Yanovitskij.⁶⁵ The calculations were fitted with the Hapke bidirectional reflection function^{1,41}

$$R_H = \frac{\bar{\omega}_H}{4} \frac{1}{\mu + \mu_0} [p_H(\theta) + H(\mu_0, \bar{\omega}_H)H(\mu, \bar{\omega}_H) - 1], \quad (18)$$

where we have omitted the shadowing term as negligibly small for sparsely distributed scatterers. In Eq. (18), $\bar{\omega}_H$ is model single-scattering albedo, μ_0 and μ are cosines of the angles of light incidence and reflection, respectively, as measured from the normal to the surface, θ is the scattering angle (angle between incident and reflected light), the function

$$H(x, \bar{\omega}_H) = \frac{1 + 2x}{1 + 2x(1 - \bar{\omega}_H)^{1/2}} \quad (19)$$

approximates the Chandrasekhar H -function for isotropic scattering, and the function p_H describes the contribution of the first-order scattering and is usually chosen to be a single-peaked Henyey-Greenstein phase function characterized by the model asymmetry parameter g_H :

$$p_H(\theta) = \frac{1 - g_H^2}{(1 - 2g_H \cos \theta + g_H^2)^{3/2}}. \quad (20)$$

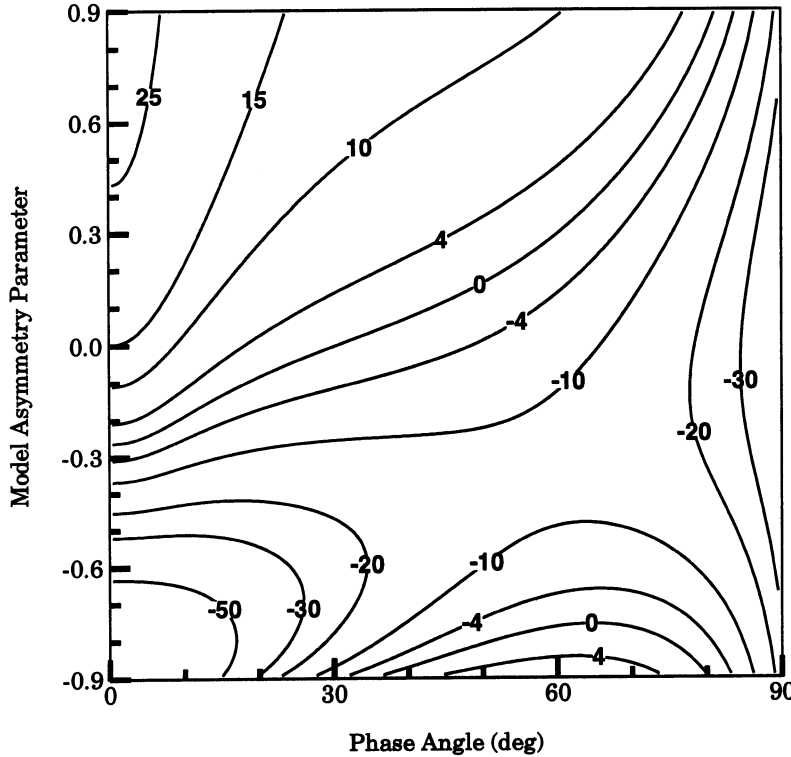


Fig. 10. Contour plot of the relative error ϵ as a function of the phase angle and Hapke model asymmetry parameter g_H for the case of normal incidence and oblique reflection of light and $\bar{\omega}_H = 1$ (see text). Owing to reciprocity, this figure is also relevant to the case of oblique incidence and normal reflection of light.

Thus, as mentioned above, in the Hapke model the contribution of photons scattered more than once is approximated by that of isotropic scatterers. The fit of the Hapke reflection function R_H to the rigorously calculated reflection function R is characterized by the relative error

$$\epsilon = \frac{R - R_H}{R_H} \times 100\%. \quad (21)$$

In Fig. 10, the error ϵ is shown as a function of the reflection angle (or, equivalently, the phase angle which is equal to the angle between the direction of light reflection and the direction opposite to the direction of light incidence, i.e., $180^\circ - \theta$) and the model asymmetry parameter g_H for the case of normal incidence of light and model single-scattering albedo $\bar{\omega}_H = 1$. Note that owing to reciprocity, this figure is also relevant to the case of oblique illumination and normal reflection. It is seen that none of the model asymmetry parameters g_H from the interval $[-0.9, 0.9]$ provide an acceptable fit. However, as shown in Fig. 11, an excellent fit for angles of reflection from 0° up to 80° is provided by the model single-scattering albedo $\bar{\omega}_H = 0.996$ and asymmetry parameter $g_H = -0.4$. (Figure 12 shows that further decrease of the model single scattering albedo makes the fit worse.) Thus, the actual, rigorously computed reflection function for strongly forward scattering particles with the asymmetry parameter of about 0.82 is well represented by the Hapke bidirectional reflection function with the model asymmetry parameter $g_H = -0.4$ corresponding to moderately backscattering particles. This result can easily be understood. Indeed, since the Hapke term describing the contribution of multiply scattered photons can substantially underestimate the real multiple-scattering contribution in the backward direction,³⁷ this underestimation must be compensated for by artificially enhancing the single-scattering phase function in the backscattering direction and, therefore, decreasing the asymmetry parameter. The fact that the retrieved model single-scattering albedo $\bar{\omega}_H$ is smaller than the actual one results in an even bigger error in the retrieved asymmetry parameter g_H . In addition, although the rigorous radiative transfer computations have been performed for a semi-infinite layer with a flat boundary, the residual differences at phase angles greater than 80° (Fig. 11), resulting from the use of the Hapke approximate

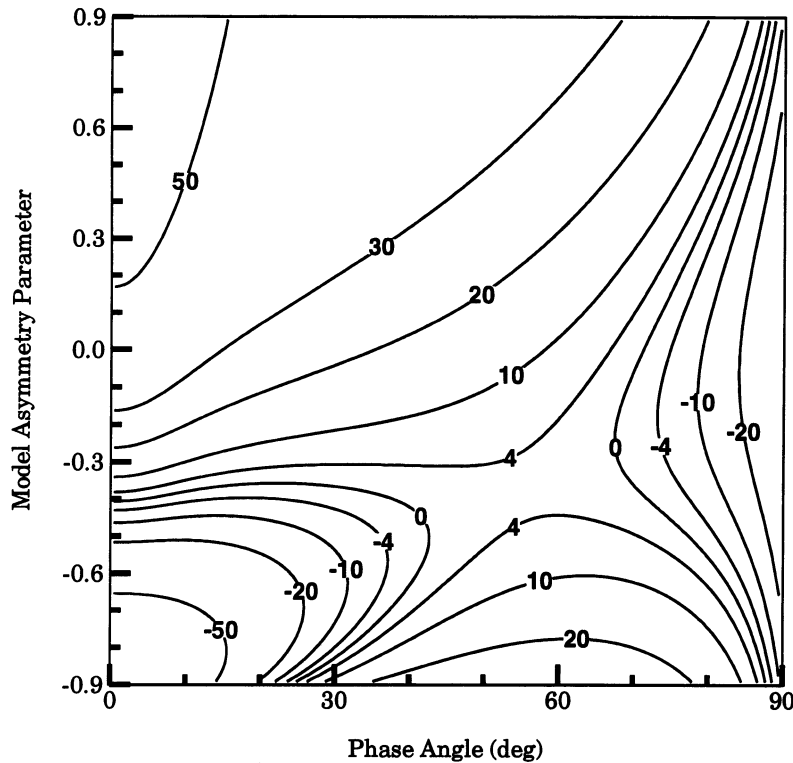


Fig. 11. As in Fig. 10, but for $\bar{\omega}_H = 0.996$.

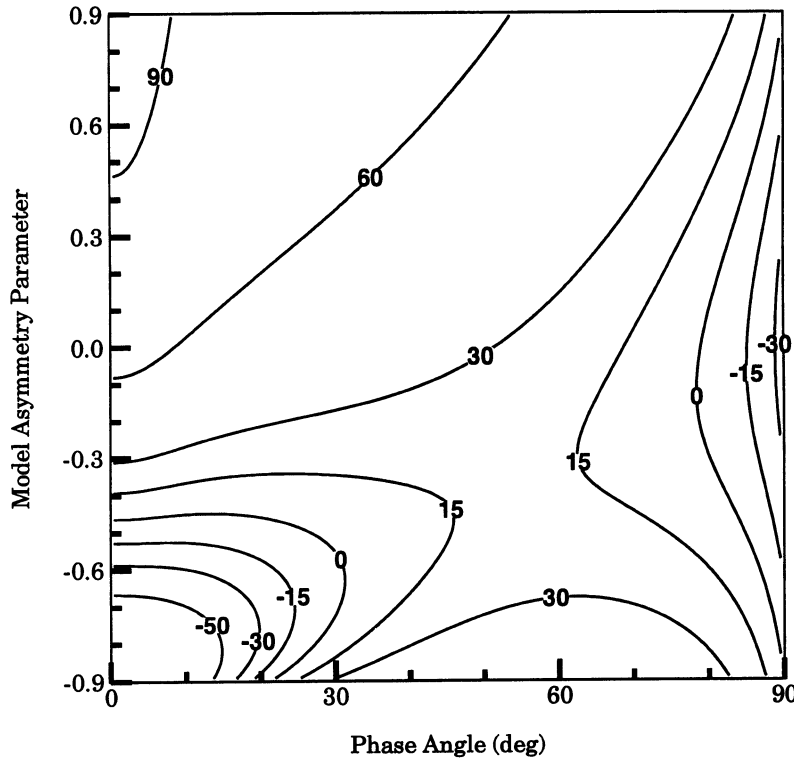


Fig. 12. As in Fig. 10, for $\bar{\omega}_H = 0.99$.

reflection function, could, apparently, be misinterpreted by artificially introducing a nonzero macroscopic surface roughness.³

Figures 13–15 show analogous computations for the mirror geometry of light reflection, when both incident and reflected beams lie in a plane perpendicular to the surface and the phase angle is equal to twice the angle of incidence and varies from 0° (normal incidence and normal reflection) to 180° (grazing incidence and grazing reflection). We see that in the case of conservative scattering ($\bar{\omega}_H = 1$, Fig. 13) none of the Hapke asymmetry parameters can provide an acceptable fit for the entire range of phase angles, and that artificially introducing absorption (Figs. 14 and 15) only increases the errors. The errors are especially big at the forward-scattering direction (phase angles larger than approximately 120°), which is not surprising. Indeed, the actual contribution of n times forward-scattered photons is proportional to the n th power of the forward-scattering value of the phase function, whereas in the Hapke reflection function it is proportional only to the first power (higher-order scattering is assumed to be isotropic). As a result, the Hapke reflection function grossly underestimates the forward-reflected intensity. Only at exactly the grazing incidence and reflection (phase angle = 180°), when only the single-scattered photons contribute to the reflected intensity,⁶⁶ the errors are small for $g_H \approx 0.85$.

It is well known that it is multiple scattering which makes clouds backscattering despite forward-scattering phase functions of cloud particles.⁶⁶ It follows from our computations that (1) the same is true for regolithic, soil, and snow surfaces and (2) it is the approximate Hapke reflection function which makes the model phase function backscattering. The latter conclusion is well illustrated by laboratory measurements and model computations by Hapke and Wells.⁵⁴ It is known from the radiative transfer theory that decreasing absorption and, thus, increasing the single-scattering albedo drastically increases the amount of multiple scattering (the contribution of the n th-order scattering is proportional to the n th power of the single-scattering albedo⁶⁶) and, therefore, reflectivity. Such a dramatic increase of reflectivity with decreasing absorption is indeed seen in Figs. 3–5 in Ref. 54. However, because of the inability of the Hapke isotropic multiple-scattering term to adequately represent the real multiple-scattering contribution, this

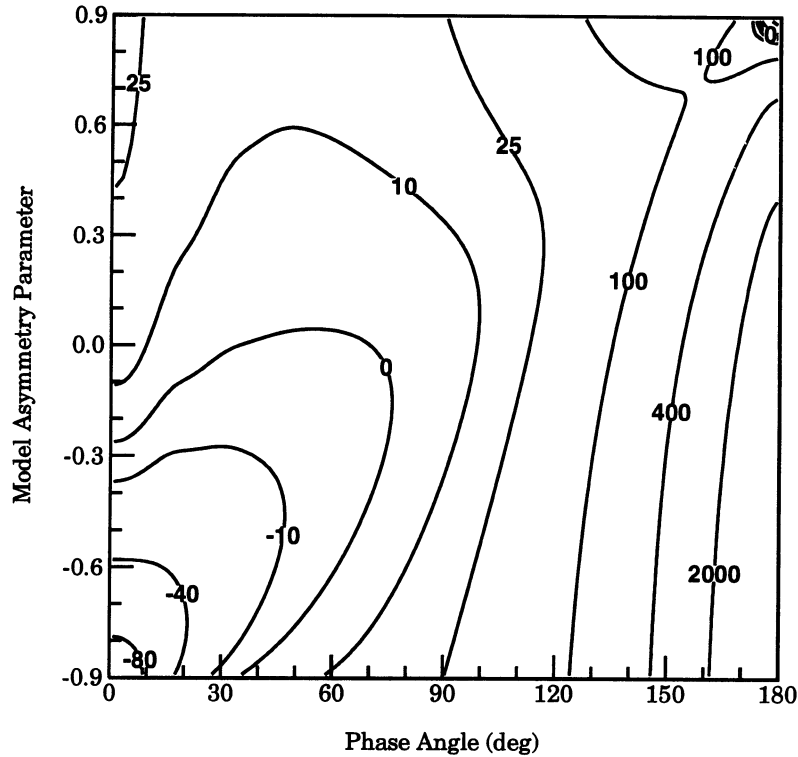


Fig. 13. Contour plot of the relative error ϵ as a function of the phase angle and Hapke model asymmetry parameter g_H for the case of the mirror geometry of light reflection and $\bar{\omega}_H = 1$ (see text).

increase of reflectivity is misinterpreted in terms of steeply enhancing the single-scattering phase function in the backscattering direction. This makes the phase function for almost nonabsorbing, transparent glass particles backscattering (model asymmetry parameter $g_H = -b/3 = -0.24$ for $37\text{--}74\text{ }\mu\text{m}$ particles), which does not seem physically realistic.

4. CONCLUDING REMARKS

In this paper, we have used a dense-medium light-scattering theory based on introducing the static structure factor to compute asymmetry parameters of the single-scattering phase function for densely packed particles. Our calculations show that the effects of packing density do not change the asymmetry parameter significantly for particles much smaller and much larger than the wavelength of light. However, asymmetry parameters for particles with radius-to-wavelength ratios from roughly 0.1 to roughly 1 can be changed substantially and may even become negative. By definition, the dense-medium single-scattering phase function accurately represents only the first-order-scattering contribution to the intensity reflected by a scattering layer. However, it apparently can be used in the radiative transfer equation to compute the full reflected intensity for nonabsorbing and moderately absorbing particles. For strongly absorbing particles with sizes much greater than the wavelength, Monte Carlo ray-tracing techniques may give good results.

Since our computations are based on a solid physical background, they can be used to examine the physical relevance of approximate reflection functions pretending to adequately describe multiple light scattering. We have shown that the negative asymmetry parameters obtained with the Hapke bidirectional reflection function are, most likely, physically irrelevant. However, this result is not the only evidence that something may be wrong with the Hapke bidirectional reflection function. We have also examined the Hapke reflection function vs rigorous numerical solutions of the radiative transfer equation for independently scattering particles, in which case the radiative transfer theory gives exact results. We have found that the use of the Hapke reflection function to reconstruct the original asymmetry parameter can give significant errors. Specifically, whereas

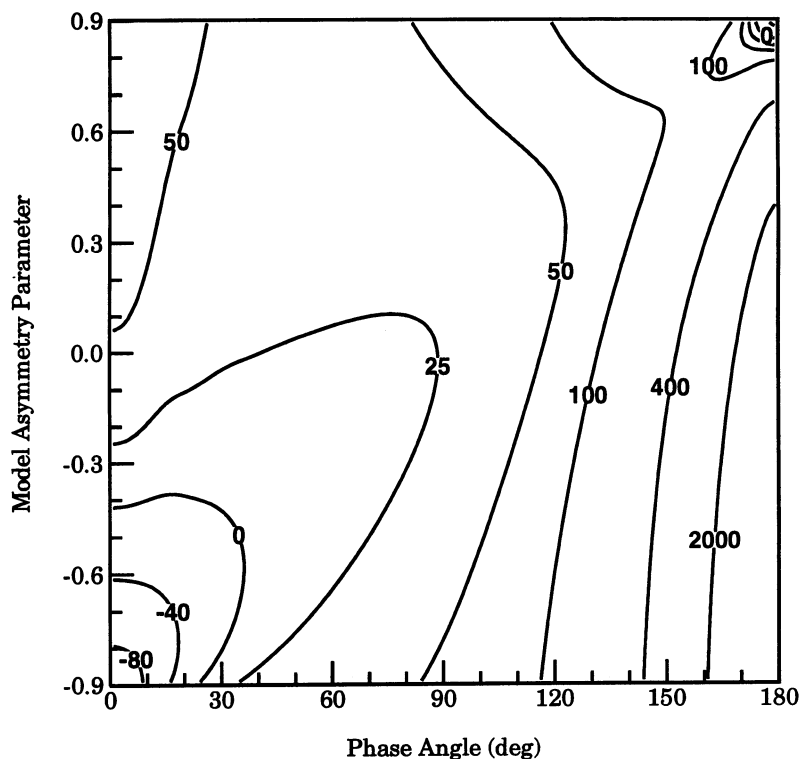


Fig. 14. As in Fig. 13, but for $\bar{\omega}_H = 0.996$.

the original strongly forward-scattering phase function used in numerically solving the radiative transfer equation had an asymmetry parameter $g = 0.82$, the retrieved model asymmetry parameter was $g_H = -0.4$, corresponding to a moderately backscattering phase function. The retrieved model asymmetry parameter is physically irrelevant and is an artifact of using several unjustified approximations combined with the ill-conditionality of the inverse scattering problem.

The Hapke bidirectional reflection function and a number of similar approximate models (e.g., Ref. 67 and references therein) have been widely used to analyze photometric observations of the Earth and planetary surfaces and planetary atmospheres and have been found to be able to fit the data well with a small number of free model parameters. In this regard, these models may be considered a useful interpolation tool (e.g., Helfenstein et al¹). However, these models have not been verified yet vs results of controlled laboratory experiments, when all physical parameters of the scattering medium (i.e., particle size distribution, shape, refractive index, and filling factor) are measured along with measuring the medium reflectance properties. It is important to note that the Hapke theory does not even contain such a crucial physical parameter as refractive index, thus making practically impossible its physical validation. So far, the Hapke bidirectional reflection function has been compared with remote photometric observations and what can be called “laboratory observations”. The latter means that only the reflectivity of a scattering medium is measured in laboratory without explicitly specifying the principal physical parameters of the scatterers.⁶⁸ Good fit of model computations to observational and laboratory data has usually been considered an evidence of the adequacy of the Hapke reflection function. However, as demonstrated above, the formal fit of model computations to observational data does not necessarily mean that the values of the model parameters represent exact and physically relevant values of specific physical properties of the scattering particles (cf. Refs. 68–70). To be relevant, a model of light scattering by regolithic, soil, or snow particles must have a solid physical background and be validated vs results of controlled laboratory experiments. Of course, real controlled laboratory experiments may be replaced by controlled “theoretical” experiments, which means that a more rigorous theory (e.g., the conventional radiative transfer theory for independent scatterers or densely packed nonabsorbing or moderately absorbing particles and Monte Carlo ray-tracing for

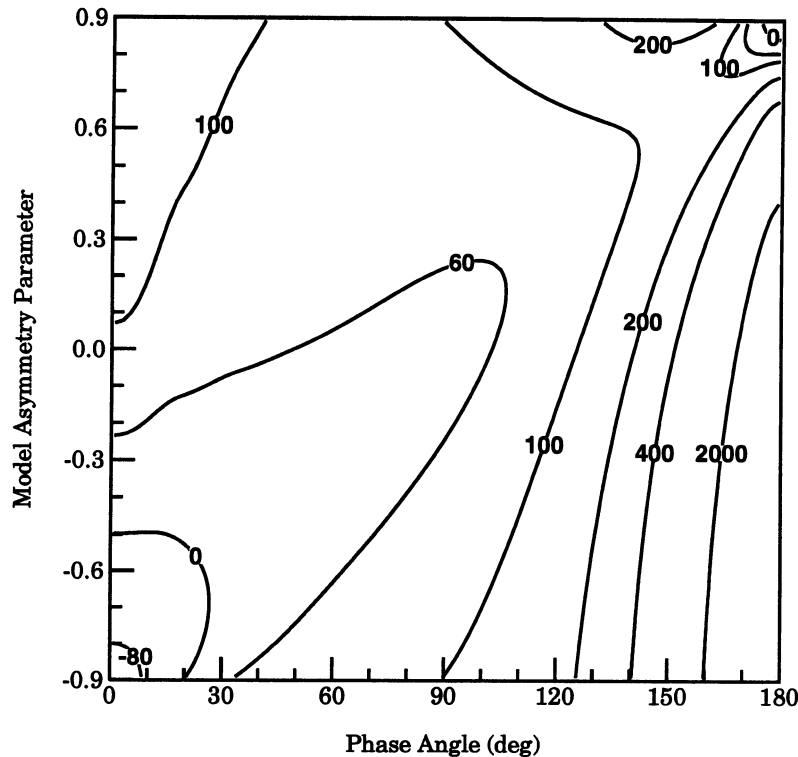


Fig. 15. As in Fig. 13, for $\bar{\omega}_H = 0.98$.

big, strongly absorbing particles) is used to produce benchmark numbers. Such a controlled “theoretical” experiment performed in Section 3 shows that the Hapke reflection function can be grossly inconsistent with rigorous numerical solutions of the radiative transfer equation.

Note added in proof—Our discussion would be incomplete without noting that in Ref. 49 rigorous numerical solutions of the (vector) radiative transfer equation were successfully used to interpret polarimetric observations of the Martian surface.

Acknowledgements—I am grateful to L. D. Travis for a discussion which initiated this study. This work was supported in part by the Earth Observing System Project managed by Goddard Space Flight Center in providing for the Earth Observing Scanning Polarimeter instrument analysis and algorithm development.

REFERENCES

1. P. Helfenstein and J. Veverka, in *Asteroids II*, R. P. Binzel, T. Gehrels, and M. S. Matthews, eds., p. 557, University of Arizona Press, Tucson (1989).
2. A. Dollfus, M. Wolff, J. E. Geake, D. F. Lupishko, and L. M. Dougherty, in *Asteroids II*, R. P. Binzel, T. Gehrels, and M. S. Matthews, eds., p. 594, University of Arizona Press, Tucson (1989).
3. E. Bowell, B. Hapke, D. Domingue, K. Lumme, J. Peltoniemi, and A. Harris, in *Asteroids II*, R. P. Binzel, T. Gehrels, and M. S. Matthews, eds., p. 524, University of Arizona Press, Tucson, AZ (1989).
4. H. C. van de Hulst, *Light Scattering by Small Particles*, Wiley, New York, NY (1957).
5. C. F. Bohren and D. R. Huffman, *Absorption and Scattering of Light by Small Particles*, Wiley, New York, NY (1983).
6. C. F. Bohren and B. R. Barkstrom, *J. geophys. Res.* **79**, 4527 (1974); C. F. Bohren and R. L. Beschta, *Cold Regions Sci. Technol.* **1**, 47 (1979).
7. W. J. Wiscombe and S. G. Warren, *J. Atmos. Sci.* **37**, 2712 (1980).
8. S. G. Warren and W. J. Wiscombe, *J. Atmos. Sci.* **37**, 2734 (1980); S. Warren, *Rev. Geophys. Space Phys.* **20**, 67 (1982).
9. S. G. Warren, W. J. Wiscombe, and J. F. Firestone, *J. geophys. Res.* **95**, 14717 (1990).
10. J. Dozier, in *Theory and Applications of Optical Remote Sensing*, G. Asrar, ed., p. 527, Wiley, New York, NY (1989); A. W. Nolin and J. Dozier, *Rem. Sens. Environ.* **44**, 231 (1993).
11. R. M. Goody and Y. L. Yung, *Atmospheric Radiation*, Oxford University Press (1989).
12. A. Lacis, J. Hansen, and M. Sato, *Geophys. Res. Lett.* **19**, 1607 (1992).
13. F. P. Fanale, J. R. Salvail, D. L. Matson, and R. H. Brown, *Icarus* **88**, 193 (1990).

14. B. Pinty, M. M. Verstraete, and R. E. Dickinson, *Rem. Sens. Environ.* **27**, 273 (1989).
15. R. Balescu, *Equilibrium and Nonequilibrium Statistical Mechanics*, Wiley, New York, NY (1975).
16. V. Twersky, *JOSA* **73**, 313 (1983).
17. L. Tsang and J. A. Kong, *Radio Sci.* **18**, 1260 (1983).
18. S. M. Rytov, Yu. A. Kravtsov, and V. I. Tatarskii, *Statistical Radiophysics*, Vol. 2, Nauka, Moscow (1978); English translation: Springer, Berlin (1989).
19. P. E. Wolf, G. Maret, E. Akkermans, and R. Maynard, *J. Phys. (Paris)* **49**, 63 (1988); S. Fraden and G. Maret, *Phys. Rev. Lett.* **65**, 512 (1990).
20. P. M. Saulnier, M. P. Zinkin, and G. H. Watson, *Phys. Rev. B* **42**, 2621 (1990).
21. M. I. Mishchenko, *Astrophys. Space Sci.* **194**, 327 (1992).
22. T. Ishida, H. Ando, and M. Fukuhara, *Rem. Sens. Environ.* **38**, 173 (1991).
23. J. E. Hansen and L. D. Travis, *Space Sci. Rev.* **16**, 527 (1974).
24. W. J. Wiscombe, *Appl. Opt.* **19**, 1505 (1980).
25. J. D. Cartigny, Y. Yamada, and C. L. Tien, *J. Heat Transfer* **108**, 608 (1986).
26. K. Kamiuto, *JQSRT* **43**, 39 (1990).
27. P. C. Waterman, *Phys. Rev. D* **3**, 825 (1971).
28. M. I. Mishchenko, *JOSA A* **8**, 871 (1991).
29. M. I. Mishchenko, *Appl. Opt.* **32**, 4652 (1993).
30. A. Mugnai and W. J. Wiscombe, *Appl. Opt.* **25**, 1235 (1986).
31. M. B. van der Mark, M. P. van Albada, and A. Lagendijk, *Phys. Rev. B* **37**, 3575 (1988).
32. M. I. Mishchenko and J. M. Dlugach, *Planet. Space Sci.* **41**, 173 (1993).
33. M. I. Mishchenko, *Astrophys. J.* **411**, 351 (1993).
34. L. Tsang, K. H. Ding, and B. Wen, in *Progress in Electromagnetic Research 3*, J. A. Kong, ed., p. 75, Elsevier, New York, NY (1990).
35. M. P. van Albada, M. B. van der Mark, and A. Lagendijk, *J. Phys. D* **21**, S28 (1988).
36. M. I. Mishchenko, *Phys. Rev. B* **44**, 12597 (1991).
37. J. D. Goguen, *Icarus*, submitted (1993).
38. Y. Kuga, F. T. Ulabi, T. F. Haddock, and R. D. DeRoo, *Radio Sci.* **26**, 329 (1991); F. T. Ulabi, T. F. Haddock, R. T. Austin, and Y. Kuga, *Radio Sci.* **26**, 343 (1991).
39. J. I. Peltoniemi and K. Lumme, *JOSA A* **9**, 1320 (1992).
40. K. Lumme and E. Bowell, *Astron. J.* **86**, 1694 (1981).
41. B. Hapke, *J. geophys. Res.* **86**, 3039 (1981).
42. A. J. Verbiscer and J. Veverka, *Icarus* **82**, 336 (1989).
43. B. Buratti, F. Wong, and J. Mosher, *Icarus* **84**, 203 (1990).
44. A. Verbiscer, P. Helfenstein, and J. Veverka, *Nature* **347**, 162 (1990).
45. B. J. Buratti, *Icarus* **92**, 312 (1991).
46. P. Lee, P. Helfenstein, J. Veverka, and D. McCarthy, *Icarus* **99**, 82 (1992).
47. R. H. Zerull, *Beitr. Phys. Atmos.* **49**, 168 (1976).
48. D. L. Jaggard, C. Hill, R. W. Shorthill, D. Stuart, M. Glantz, F. Rosswog, B. Taggart, and S. Hammond, *Atmos. Environ.* **15**, 2511 (1981).
49. J. F. de Haan, Ph.D. thesis, Free University, Amsterdam (1987).
50. W. J. Wiscombe and A. Mugnai, *Appl. Opt.* **27**, 2405 (1988).
51. P. Stamnes, Ph.D. thesis, Free University, Amsterdam (1989).
52. F. Kuik, Ph.D. thesis, Free University, Amsterdam (1992).
53. A. Macke, *Appl. Opt.* **32**, 2780 (1993).
54. B. Hapke and E. Wells, *J. geophys. Res.* **86**, 3055 (1981).
55. A. Verbiscer, P. Helfenstein, and J. Veverka, *Nature* **347**, 162 (1990).
56. A. McGuire and B. Hapke, *Proc. Lunar Planet. Sci. Conf.* **21**, 767 (1990).
57. J. C. Oelund and N. J. McCormick, *JOSA A* **2**, 1972 (1985).
58. N. J. McCormick, *Nucl. Sci. Engng* **112**, 185 (1992).
59. K. Kamiuto, *JQSRT* **46**, 309 (1991).
60. B. Hapke, *Theory of Reflectance and Emittance Spectroscopy*, Cambridge University Press (1993).
61. J. E. Hansen and J. W. Hovenier, *J. Atmos. Sci.* **31**, 1137 (1974).
62. W. A. de Rooij and C. C. A. H. van der Stap, *Astron. Astrophys.* **131**, 237 (1984).
63. O. A. Volkovitskiy, L. N. Pavlova, and A. G. Petrushin, *Izvestiya, Atmos. Ocean. Phys.* **16**, 98 (1980).
64. V. V. Sobolev, *Light Scattering in Planetary Atmospheres*, p. 31, Eq. (2.37), Pergamon Press, Oxford (1975).
65. J. M. Dlugach and E. G. Yanovitskij, *Icarus* **22**, 66 (1974).
66. H. C. van de Hulst, *Multiple Light Scattering*, Academic Press, New York, NY (1980).
67. S. P. Ahmad and D. W. Deering, *J. geophys. Res.* **97**, 18867 (1992).
68. K. Muinonen, Ph.D. thesis, University of Helsinki (1990).
69. B. Pinty and M. M. Verstraete, *Remote Sens. Environ.* **41**, 155 (1992).
70. J. I. Peltoniemi, Ph.D. thesis, University of Helsinki (1993).